

# 1 Uncertainty assessment for on-machine tool 2 measurement: an alternative approach to the ISO 3 15530-3 technical specification

4 Unai Mutilba<sup>1,\*</sup>, Eneko Gomez-Acedo<sup>1</sup>, Alejandro Sandá<sup>2</sup>, Ibon Vega<sup>2</sup> and Jose A. Yagüe-Fabra<sup>3</sup>

5 <sup>1</sup> Department of Mechanical Engineering, IK4-Tekniker, Eibar 20600, Spain; eneko.gomez-acedo@tekniker.es  
6 (E.G.-A.)

7 <sup>2</sup> Department of Production Engineering, IK4-Tekniker, Eibar 20600, Spain; alejandro.sanda@tekniker.es  
8 (A.S.); ibon.vega@tekniker.es (I.V.)

9 <sup>3</sup> I3A, Universidad de Zaragoza, Zaragoza 50018, Spain; jyague@unizar.es

10 \* Correspondence: unai.mutilba@tekniker.es; Tel.: +34-636-994-351

11 Received: date; Accepted: date; Published: date

12 **Abstract:** Touch probes are commonly employed in new machine tools (MTs), and enable  
13 machining and measuring processes to occur on the same MT. They offer the potential to measure  
14 components, either during or after the machining process, providing traceability of the quality  
15 inspection on the MT. Nevertheless, there are several factors that affect measurement accuracy on  
16 shop-floor conditions, such as MT geometric errors, temperature variation, probing system,  
17 vibrations and dirt. Thus, the traceability of a measurement process on an MT is not guaranteed  
18 and measurement results are therefore not sufficiently reliable for self-adapting manufacturing  
19 processes. The current state-of-the-art approaches employ a physically calibrated workpiece to  
20 realise traceable on-MT measurement according to the ISO 15530-3 technical specification, but it  
21 has a significant limitation in that it depends on a physical workpiece to understand the  
22 performance of the systematic error contributor ( $u_b$ ). To this end, the aim of this paper is to  
23 propose an alternative methodology for on-MT uncertainty assessment without using a calibrated  
24 workpiece. The proposed approach is based on a volumetric error mapping of the MT prior to the  
25 measurement process, which provides an understanding of how the systematic error contributor  
26 ( $u_b$ ) performs. An experimental exercise is performed for a medium-size prismatic component  
27 according to the VDI 2617-11 guideline, and the results are compared with the ISO 15530-3  
28 technical specification.

29 **Keywords:** uncertainty budget; on-machine tool measurement; traceability; uncertainty  
30

---

## 31 1. Introduction

32 The development of flexible manufacturing processes for high-quality products at low cost is  
33 one of the main research objectives in the field of production technology [1]. The quality inspection  
34 of high-value components usually takes place on coordinate measuring machines (CMMs), either  
35 beside the production line or in an isolated measurement room, so the manufacturing process is  
36 interrupted and transportation, handling and the loss of the original manufacturing setup influence  
37 the workpiece quality [2] and the overall equipment effectiveness (OEE). The high investment  
38 required for a CMM and the above-mentioned limitations show the need for a machine tool (MT)  
39 integrated traceable measuring process.

40 Although on-MT measurement can provide advantages for more flexible and intelligent  
41 manufacturing processes, there are also some limitations. The main limitation is that MT time is  
42 more expensive than CMM time, so measurements that are executed on an MT should clearly add  
43 value to the manufacturing process. Here, it is particularly relevant to determine critical component  
44 dimensions and measure them on the MT in order to ensure zero-defect manufacturing processes  
45 [3].

46 The current manufacturing scenario shows that dimensional measurements are already being  
47 employed for on-MT measurements at different stages of the manufacturing cycle, mainly because  
48 the technology to perform a measurement, either touch-trigger probes (TTPs) or measurement  
49 software, are already available on the MT side. There are four potential measurement scenarios  
50 where on-MT measurement adds value to the manufacturing process: a) monitoring of the MT  
51 geometry performance by employing a calibrated standard; b) workpiece set up on the MT  
52 coordinate system; c) in-process measurements to provide correction values for the manufacturing;  
53 and d) the performance of a final metrology validation of the finished product for final quality  
54 inspection as well as statistical trend analysis of the manufacturing process. Nowadays, depending  
55 on the size of the component, traceable on-MT measurement technology readiness levels (TRLs) are  
56 at different stages: While large-scale manufacturing processes employ on-MT measurements to  
57 reduce the setup time of large components on the MT bed, medium-size aeronautic manufacturers  
58 are already performing on-MT measurement for the in-process measurement of high-value  
59 components such as aircraft engines and components, close to realising a traceable on-MT  
60 measurement.

61 From a technology point of view, the aim is to use an MT as a CMM, but there are some key  
62 differences between a CMM and an MT, mainly because CMMs are designed for measurement  
63 purposes and MTs are focused on manufacturing production. The main problem when executing a  
64 measurement on an MT is that the machining and measuring processes are performed using the  
65 same machine, and some error sources therefore cannot be distinguished if a calibration process is  
66 not realised before the measurement execution [4]. This is currently the main limitation to close the  
67 calibration chain for on-MT measurement.

68 Over the years, several standards and guidelines [5–10] have been developed in order to verify  
69 the accuracy of either MTs [11–16] or CMMs [6,7], but measurement traceability assessments for on-  
70 MT measurements are not as developed as is the case for CMMs. In this scenario, owing to the  
71 similarity between CMMs and MTs, some of the methods employed for a correct assessment of  
72 uncertainty in CMMs are being adopted for MTs. The general guide for a suitable evaluation of  
73 measurement data is given in the ISO Guide 98-3: 2008, on the expression of uncertainty in  
74 measurement (GUM) [17]. Three different approaches are considered for an uncertainty assessment  
75 on an MT [3]: a) an experimental technique according to ISO 15530-3 technical specification [8]; b) a  
76 numerical simulation-based approach, as described in the ISO 15530-4 technical specification [9];  
77 and c) an uncertainty budget method based on the VDI 2617-11 guideline [10].

78 Several research works have focused on the idea of converting an MT into a CMM. In 2010,  
79 Schmitt et al. proposed that a large MT should be employed as a comparator to measure the  
80 geometry of large scale components during the manufacturing process [18]. In 2013, Schmitt et al.  
81 also presented a study in which a specific workpiece was manufactured and calibrated on a CMM  
82 for several on-MT measurement experimental tests [1]. In this regard, Mutilba et al. reported that a  
83 research work where a calibrated workpiece was employed to assess the on-MT measurement  
84 uncertainty on a real manufacturing process for a medium-size prismatic component [4]. In 2015,  
85 Schmitt et al. went a step further, presenting an approach to determine the uncertainty assessment  
86 for on-MT measurements according to the VDI 2617-11 guideline; they defined a maximum  
87 permissible error (MPE) [7] for MTs to assess the systematic error of the on-MT measurement error  
88 budget [2]. Recently, Holub et al. presented a capability assessment for on-MT measurement  
89 assisted by an external laser interferometer [19]. Similarly, Sladek et al. reported an interesting  
90 approach for the systematic error assessment of a CMM based on the use of a laser tracer for the  
91 volumetric error mapping and compensation of geometric errors. It is an online accuracy-estimation  
92 solution based on the virtual coordinate measuring machine (VCMM) concept for CMMs [9,20–22].

93 In this context, this paper presents a methodology to perform traceable on-MT measurements  
94 without using a calibrated workpiece, performing the VDI 2617-11 guideline [10]. The approach  
95 aims to perform the systematic error ( $u_b$ ) assessment of on-MT measurements by means of a  
96 previous volumetric error mapping of the MT using laser tracer technology.

97 Finally, an experimental exercise was performed on a three linear-axis medium-size MT. It  
 98 shows that the uncertainty assessment for a medium-size prismatic component can be performed  
 99 without using a calibrated workpiece. Results have been compared to the ISO 15530-3 technical  
 100 specification [8].

## 101 2. On-machine tool measurement uncertainty budget

102 Before presenting the new approach, it is interesting to understand those uncertainty  
 103 contributors that should be considered for on-MT measurement uncertainty budget. The ISO 15530-  
 104 3 technical specification explicitly presents four uncertainty contributors that consist of all the  
 105 systematic and random errors comprising the uncertainty budget for on-MT measurement [8]:

- 106 •  $u_b$ : Standard uncertainty associated with the systematic error of the measurement  
 107 process.
- 108 •  $u_p$ : Standard uncertainty associated with the measurement procedure.
- 109 •  $u_{cal}$ : Standard uncertainty associated with the uncertainty of the workpiece calibration.
- 110 •  $u_w$ : Standard uncertainty associated with material and manufacturing variations.

111 Thus, the standard uncertainty of the measurement system ( $u_{MS}$ ) is given by the quadrature  
 112 sum of every uncertainty contributor, according to the formula expressed in Equation 1. In  
 113 addition, the expanded measurement uncertainty of the measurement system ( $U_{MS}$ ) is assessed by  
 114  $U_{MS} = k \times u_{MS}$  for a coverage factor of  $k=2$ , as expressed in Equation 2. For the systematic error ( $u_b$ )  
 115 contributor, different approaches are employed to assess it. If the measurement result is not  
 116 corrected by the systematic error ( $b$ ), the error fully contributes to the uncertainty, so  $u_b = b$ . Thus:

$$117 \quad u_{MS} = \sqrt{u_p^2 + u_{cal}^2 + b} \quad (1)$$

$$118 \quad U_{MS} = k * u_{MS} \quad (2)$$

119 With respect to the ISO 15530-3 technical specification, the uncertainty  $u_p$  is given by the  
 120 maximum standard deviation of every measurement performed on the workpiece; therefore, it uses  
 121 the experimental (type A) approach. The systematic error is defined as the difference between the  
 122 mean value of the on-MT measurement and the calibrated value, and the calibration uncertainty is  
 123 given by the workpiece's features calibration on a CMM. Both contributors are evaluated using the  
 124 type B method. Further, if variations of form errors and roughness owing to fluctuating  
 125 manufacturing processes and material properties are considered within their required limits, the  $u_w$   
 126 contribution is considered as insignificant [8]. In this case,  $u_w$  is considered negligible, so it is not  
 127 introduced in Equation 1.

128 For the VDI 2617-11 guideline, the determination of the on-MT measurement uncertainty is  
 129 determined using an uncertainty budget. Here, each uncertainty source and its magnitude on the  
 130 measurement result is considered. In this case, the error sources are as follows [2]:

- 131 • The geometric error of the MT and its repeatability.
- 132 • Probing system.
- 133 • Temperature: MT structure, surroundings, and workpiece.
- 134 • Workpiece under measurement: Temperature and clamping.
- 135 • Measurement procedure.
- 136 • Geometric error mapping technique.

137 Those error sources comprise systematic and random errors for the on-MT uncertainty budget  
 138 [23]. The result is the on-MT measurement uncertainty for a 95% confidence level.

139 Similar to the ISO 15530-3 technical specification, the systematic error contributor ( $u_b$ ) on the  
 140 VDI 2617-11 guideline is affected by the following error sources: geometric error of the MT, probing  
 141 system, workpiece under measurement, measurement procedure, and geometric error mapping  
 142 technique. The random contributor ( $u_p$ ) comprises the MT repeatability, touch probe repeatability,  
 143 and temperature variation for the measurement scenario. For the experimental approach presented  
 144 below, the measurement procedure and the workpiece under measurement have not been  
 145 considered for the uncertainty budget because an easy-to-measure medium-size prismatic  
 146 component was measured. Moreover, negligible deformations occur during the clamping process.  
 147 In addition, the probing system characterisation and the uncertainty of the MT volumetric error  
 148 mapping technique are within  $2 \mu\text{m}$ . Thus, the uncertainty budget exercise focuses on major  
 149 uncertainty contributors. In this manner, the geometric error of the MT is considered as the main  
 150 error source within the systematic contributor ( $u_b$ ), and the effect of the temperature on the  
 151 measurement scenario and MT repeatability are highlighted as the main random error contributors  
 152 ( $u_p$ ).

153 Considering those major uncertainty error contributors, this study adopts the random error  
 154 characterisation, which performed on the ISO 15530-3 technical specification and which does not  
 155 require a calibrated workpiece to understand how ( $u_p$ ) performs. For the systematic error  
 156 contributor ( $u_b$ ), Schmitt et al. presented an approach where an MPE value was defined for an MT.  
 157 Their approach was validated within stable temperature conditions, but they proposed further  
 158 research for unstable conditions because an unstable status causes gradients inside the structure,  
 159 and the induced deviations are hard to simulate or predict [2]. Considering such limitations, a  
 160 volumetric error mapping of the MT is performed immediately before the on-MT measurement  
 161 process execution for the systematic error characterisation. Thus, the geometric error of each contact  
 162 point is known, and the systematic error contributor ( $u_b$ ) can therefore be assessed. This research  
 163 work does not apply the systematic error value correction, so the error fully contributes to the  
 164 uncertainty budget, as in Equation 1.

### 165 3. Methodology for on-MT uncertainty assessment without a calibrated workpiece

166 A new methodology is proposed to perform the on-MT uncertainty assessment without a  
 167 calibrated workpiece:

- 168 • For the systematic error contributor ( $u_b$ ), a volumetric error mapping of the MT is  
 169 performed immediately before the on-MT measurement. Thus, the geometric error of each  
 170 point is known for the working volume of the machine, which is the main contributor to the  
 171 systematic error of the on-MT measurement. Once the on-MT measurement is performed,  
 172 measurement contact points are registered, and the geometric error of every point is  
 173 obtained from the volumetric error mapping. Thus, every measured feature is fitted again  
 174 while considering the geometric error of each contact point. The difference between the  
 175 feature characteristics before and after the second fitting exercise is the systematic error to  
 176 be considered on the error budget. Figure 1 shows the flow chart for the systematic error  
 177 characterisation.
- 178 • The systematic error originating from the tactile probe could also be considered for the  
 179 systematic error contributor ( $u_b$ ). Thus, as explained by Mutilba et al. [4] if a reliable  
 180 calibration of the probing system is performed every time the tactile probe is mounted on  
 181 the MT spindle, this contributor becomes negligible. However, if the calibration process is  
 182 not executed correctly or if the uncertainty contributor is not sufficiently small ( $< 1 \mu\text{m}$  for  
 183 small MT and  $< 3 \mu\text{m}$  for large MT) the tactile probe systematic error should be added to  
 184 the  $u_b$  value according to the square root of the sum of squares.
- 185 • The measurement procedure uncertainty ( $u_p$ ) is performed on the workpiece to be  
 186 measured on the MT, similar to the ISO 15530-3 technical specification [8]. Thus, the

187 repeatability of the on-MT measurement is performed within the temperature range of the  
 188 measurement scenario, considering that the temperature variation is critical for this  
 189 uncertainty contributor. Therefore, several on-MT measurement cycles shall be performed  
 190 within the complete temperature range of the measurement scenario. For example, consider  
 191 an eolic hub being machined in a large MT, where the temperature variation on the  
 192 surrounding air is between 18 °C and 23 °C. The  $u_p$  contributor should be assessed by  
 193 means of repeated measurement cycles (every 15 min) on the workpiece within the  
 194 working temperature range. Equation 3 shows how to calculate the  $u_p$  contributor.

- 195 • The  $u_{cal}$  contributor is considered as the standard uncertainty associated with the  
 196 measurement uncertainty on the systematic error characterisation process.

$$197 \quad \bar{y} = \frac{1}{n} \sum_{i=1}^n y_i \quad u_p = \sqrt{\frac{1}{n-1} \sum_{i=1}^n (y_i - \bar{y})^2} \quad (3)$$

198 where:

- 199 •  $\bar{y}$  = mean value of the measurement result.  
 200 •  $y$  = measured value.  
 201 •  $n$  = number of measurement results.

202 Figure 1 shows the flow chart for the systematic error characterisation.

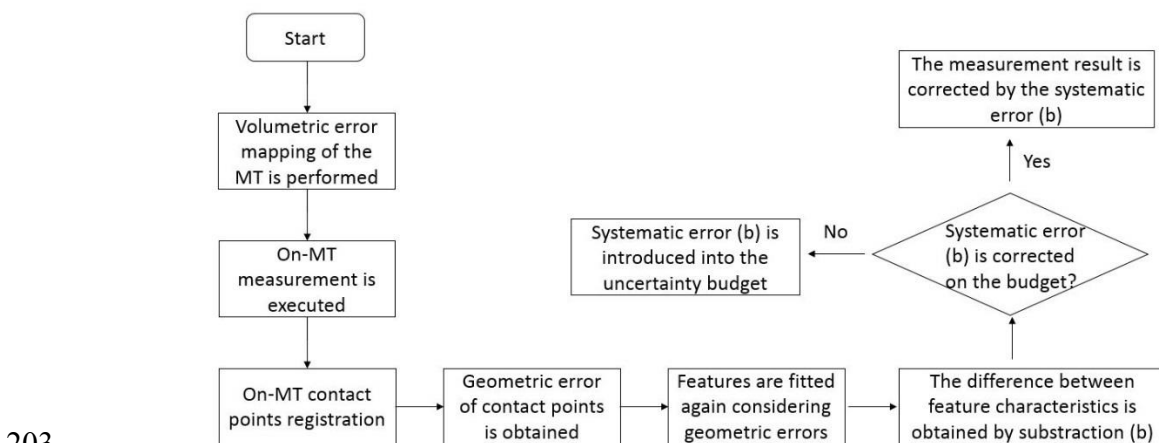


Figure 1. Systematic error assessment methodology.

205 For the geometric fitting of the measured plane and diameters, three dimensional (3D) and two  
 206 dimensional (2D) fitting equations have been employed in MATLAB [24]. This fitting exercise  
 207 considers the geometric error information of each contact point obtained in this case from the  
 208 volumetric error mapping measurement. Results obtained on each fitted feature are compared to  
 209 the initial fitting value obtained by the on-MT measurement software, so the difference between  
 210 both fittings is the systematic error to be considered on the error budget according to the VDI 2617-  
 211 11 guideline. Equation 4 shows the employed algorithm for circumference fitting; the variation of  
 212 the radius shows the roundness error.

$$213 \quad r = \sqrt{(x - x_c)^2 + (y - y_c)^2} \quad (4)$$

214 where:

- 215 •  $r$  = circumference radius.  
 216 •  $x, y$  = measured contact points (geometric error in each point is considered).  
 217 •  $x_c, y_c$  = circumference centre coordinates (to be obtained).

218 For the 3D fitting of the plane, Equation 5 shows the algorithm which was employed in this  
 219 experimental exercise. The least-squares fitting algorithm was employed to compare the flatness  
 220 error before and after considering the geometric error of the contact points [25].

$$221 \quad f(x_i, y_i, z_i) = p_1 x_i + p_2 y_i + p_3 z_i + 1 \cong 0 \quad (5)$$

222 where:

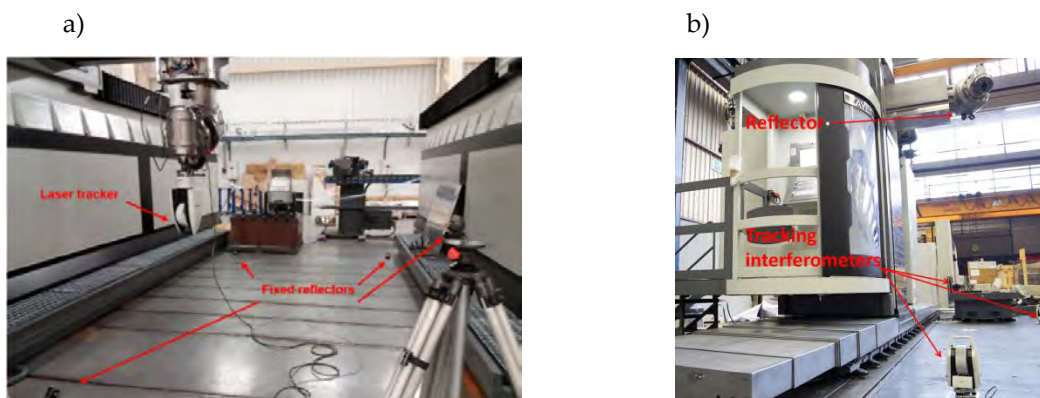
- 223 •  $p$  = plane feature parameters.
- 224 •  $x_i, y_i, z_i$  = measured contact points (geometric error in each point is considered)

#### 225 4. Technology adoption on a machine tool

226 The presented methodology requires a volumetric error mapping of the MT before performing  
 227 the on-MT measurement to characterise the geometric error of the MT as the main error source to  
 228 the systematic error ( $u_b$ ) of on-MT measurement. In this context, as explained by Nisch et al. [18],  
 229 there are two main approaches to enable a traceable measurement on MTs: a) the MT geometric  
 230 error is known at the moment when the measurement is performed through a volumetric error  
 231 mapping of the MT; and b) an external high precision metrological frame is employed to measure  
 232 and compensate for the geometric error of the MT in real time [21,22,26,27].

233 Figure 2 shows the above-mentioned two alternatives a) an MT volumetric error mapping  
 234 exercise. It shows an integrated multilateration approach reported by Mutilba et al. [30], and b) an  
 235 external high-precision metrological frame comprised of four tracking interferometers in  
 236 simultaneous mode.

237



238

239 **Figure 2.** Multilateration approaches for MT error mapping a) integrated approach , and b) external  
 240 high-precision frame with four tracking interferometers (Both measurements were performed by  
 241 IK4-TEKNIKER on a ZAYER large MT)

242 The first approach increases the process capability by a volumetric verification and  
 243 compensation of the MT, as shown in Figure 2(a). Currently, there are different options for the  
 244 volumetric error mapping of MTs [28], but they are time-consuming, mainly for large-scale MTs. In  
 245 this regard, the multilateration approach is suitable for realising such a fast performance. Schwenke  
 246 et. al. reported an approach to continuously monitor the geometric variation of a large MT on shop  
 247 floor conditions [29], and recently, Mutilba et al. reported an integrated and automatic volumetric  
 248 error mapping solution for large MTs which is executed within 30 min [30]. For the proposed  
 249 experimental approach, a volumetric error mapping of the MT under research was performed using  
 250 laser tracer NG technology in sequential mode.

251 The second approach applies an external high precision metrological frame to monitor the tool  
 252 centre point (TCP) position in real time. This option requires a line of sight between the measuring  
 253 tracking interferometers and the TCP, which cannot be ensured when the workpiece is on the MT.  
 254 The current cost of the solution is very high because four interferometers are required

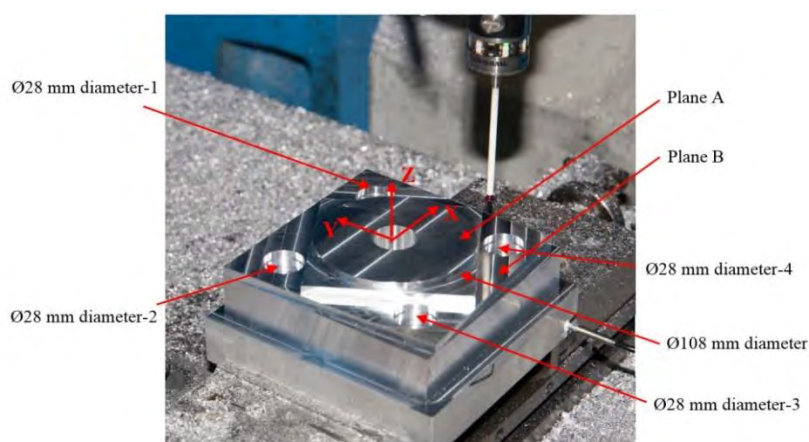


255 simultaneously. However, it offers the possibility of being self-calibrating and represents a scalable  
 256 measuring solution.

257 Currently, the first approach is under research, and according to the latest studies, with the  
 258 continued development of interferometer-based non-contact measuring technology to realise more  
 259 accurate absolute distance measurements, it will be incorporated into MTs, allowing traceable  
 260 CMM measurements in MTs [31].

## 261 5. Uncertainty budget assessment experimental exercise

262 An experimental exercise of the proposed methodology was performed using a workpiece  
 263 replica standard. The obtained results were compared to the ISO 15530-3 technical specification.  
 264 The workpiece replica standard selected for the experimental uncertainty assessment exercise is  
 265 defined at the ISO 10791-7:2014 standard [32], and it is referred as a 'Test piece ISO 10791-7, M1-  
 266 160'. A description of the measured geometry is illustrated in Figure 3.

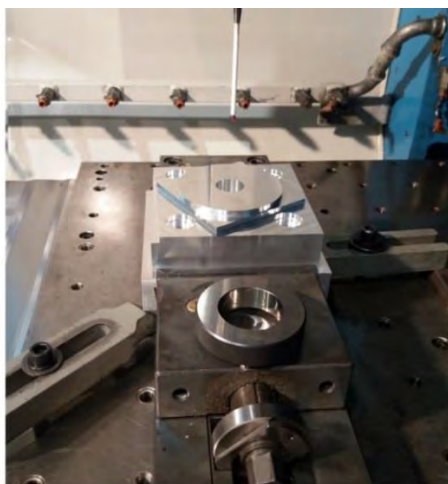
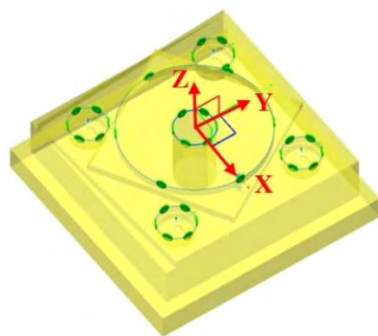


267  
 268 **Figure 3.** Workpiece replica standard with measured geometry on the experimental test.

269 A medium-size KONDIA MAXIM MT equipped with a RENISHAW OMP 400 tactile probe  
 270 and POWER INSPECT on-MT measurement software was selected to run the on-MT measurement  
 271 experimental test. The MT cutting stroke is: X = 750 mm, Y = 1000 mm and Z = 500 mm. The  
 272 computer numerical control (CNC) is a 16i-type FANUC controller. For the tactile probe calibration  
 273 on the MT spindle, a 50 mm-diameter calibrated ring was employed immediately after it was  
 274 mounted on the MT spindle. Figure 4 shows a) the measured contact points for the experimental  
 275 on-MT measurement test and b) the measurement scenario on the MT.

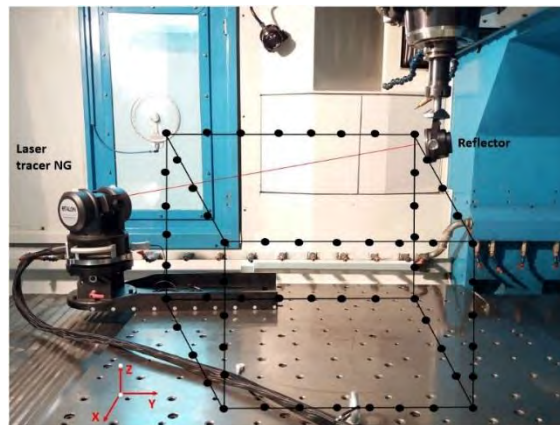
276 a)

b)



277  
 278 **Figure 4.** On-MT measurement contact points, a) General overview of the measurement strategy (contact  
 279 points in green), and b) the measurement scenario where the workpiece and the calibrated ring are shown.

280 For the systematic error contributor ( $u_b$ ) assessment, a volumetric error mapping of the MT  
 281 was performed immediately before the on-MT measurement. To do this, laser tracer technology  
 282 from ETALON AG was employed [33]. It employs a kinematic model which enables to calculate the  
 283 geometric error of any point within the measured volume from the volumetric error mapping  
 284 information, so the geometric error of the on-MT measurement contacts points was assessed in this  
 285 manner. Figure 5 shows the volumetric error mapping exercise and the measured point grid (in  
 286 black) of the MT. The laser tracer NG, which is placed on the MT table, measures the distance to the  
 287 reflector, which is fixed to the spindle, for every point comprising the point grid under the  
 288 multilateration scheme [33]. It demonstrates the technology adoption of the above-mentioned first  
 289 approach where a unique tracking interferometer is employed in sequential mode for the MT  
 290 volumetric error mapping.

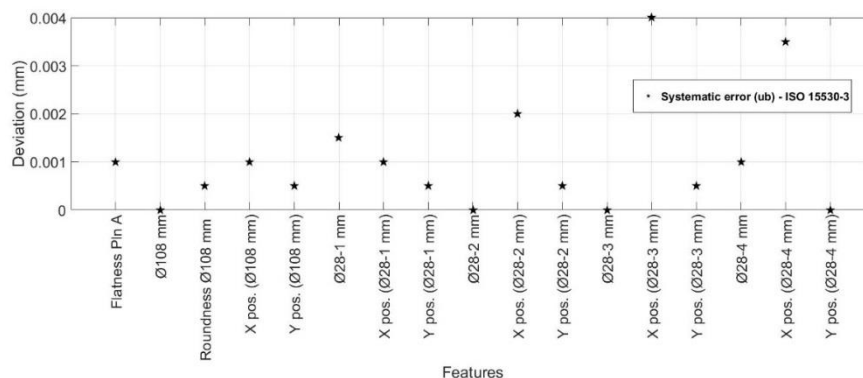


291  
 292 **Figure 5.** Volumetric error mapping of MT and measured point grid (in black).

293 The volumetric error mapping measurement was performed under a no-load condition when  
 294 the temperature on the MT side was 20 °C, with a temperature variation within 0.5 °C.

#### 295 5.1 On-MT measurement results according to ISO 15530-3 technical specification

296 The experimental on-MT measurement exercise according to the ISO 15530-3 technical  
 297 specification is explained in detail in the article: ‘Traceability of on-MT measurement: Uncertainty  
 298 budget assessment on shop floor conditions’ which was reported by Mutilba et al in 2018 [4]. Here,  
 299 the approach is to employ a CMM-calibrated workpiece replica standard to assess the on-MT  
 300 measurement uncertainty. Figure 6 shows the absolute value of the systematic error contributor ( $u_b$ )  
 301 assessed using the calibrated workpiece. All of the results are within 8  $\mu\text{m}$ .

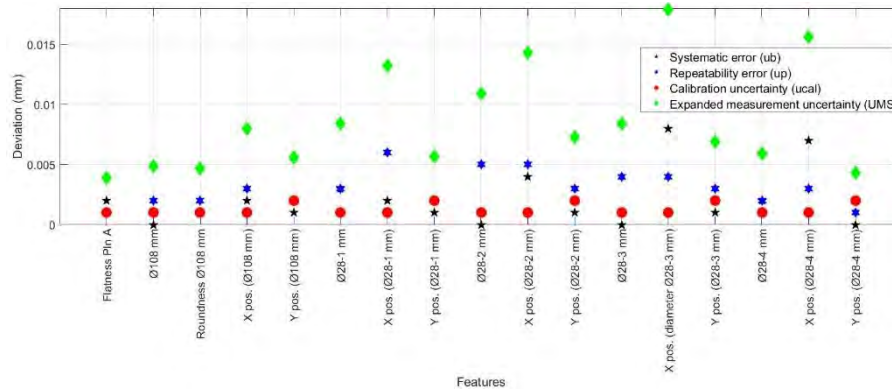


302  
 303 **Figure 6.** Systematic error ( $u_b$ ) according to ISO 15530-3 technical specification. [4]

304 The uncertainty budget of the task-specific uncertainty assessment on shop floor conditions  
 305 according to the ISO 15530-3 technical specification [4] is shown in Figure 7. The measurement  
 306 procedure uncertainty ( $u_p$ ) is on average a few micrometres larger on than the systematic error ( $u_b$ )  
 307 uncertainty, which is within 8  $\mu\text{m}$  for every measured feature. The calibration uncertainty



308 contributor ( $u_{cal}$ ) is within 2  $\mu\text{m}$  for each feature. Expanded measurement uncertainty results are  
 309 obtained by Equation 2 for a coverage factor of  $k = 2$ , where  $u_{MS}$  is given by Equation 1. As  
 310 previously mentioned, it should be considered that the systematic error ( $u_b$ ) contributor is not  
 311 corrected on the uncertainty budget, which significantly increases the expanded measurement  
 312 uncertainty ( $U_{MS}$ ) result.



313  
 314

**Figure 7.** Uncertainty budget according to ISO 15530-3 technical specification. [4]

### 315 5.2 On-MT measurement results according to VDI 2617-11 guideline

316 The main difference for the VDI 2617-11 approach is that a calibrated workpiece is not  
 317 employed to assess the systematic error uncertainty contributor ( $u_b$ ) on the uncertainty budget.  
 318 Thus, a volumetric error mapping of the MT was performed immediately before the on-MT  
 319 measurement exercise, and the TRAC-CAL software from the company ETALON AG, which  
 320 includes kinematic models for point-error determination, was used to calculate the geometric error  
 321 of each contact point for the on-MT measurement process. Figure 5 shows the volumetric error  
 322 mapping setup on the MT, and Figure 8 shows the 3D deviation result of each measured point  
 323 comprising the point grid. The simple ETALON kinematic model was employed, and was  
 324 performed by 17 components of the error, and the results are depicted in a 3D deviation-type plot.  
 325 The uncertainty for the geometric error mapping measurement is within 1  $\mu\text{m}$ . The volume of the  
 326 point grid depicted in Figure 8 is similar to the MT cutting stroke, i.e.  $X = 750 \text{ mm}$ ,  $Y = 1000 \text{ mm}$  and  
 327  $Z = 500 \text{ mm}$ .

328  
 329

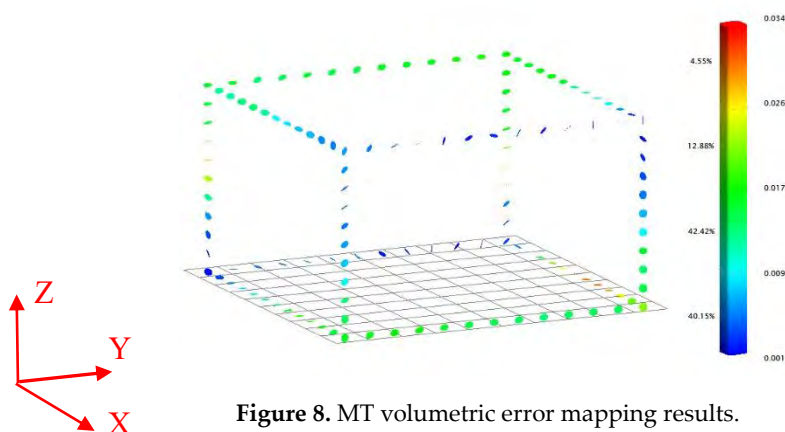
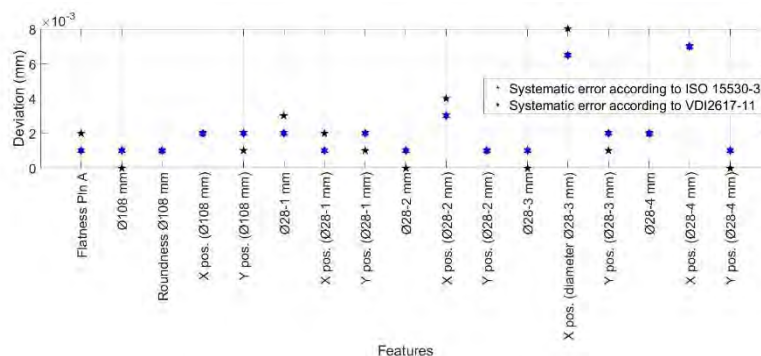


**Figure 8.** MT volumetric error mapping results.

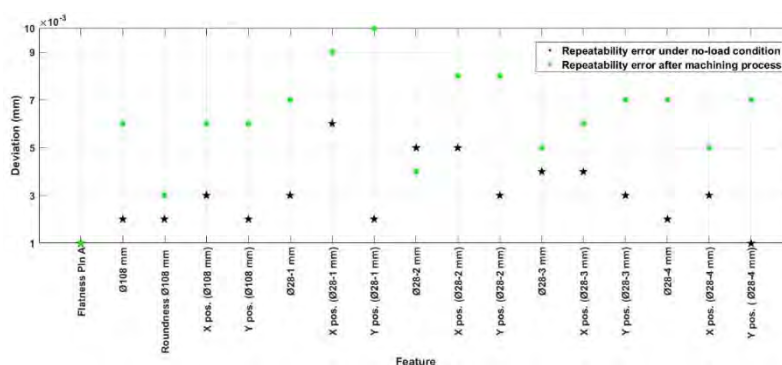
330 The MT volumetric error mapping exercise demonstrates that the geometric error is within 20  
 331  $\mu\text{m}$  for almost the entire volume of the machine. Moreover, the workpiece replica standard size is  
 332  $160 \text{ mm} \times 160 \text{ mm}$ , which means that the geometric error on the MT side that applies to the on-MT  
 333 measurement is within 5  $\mu\text{m}$ . The volumetric error mapping process also measures the MT  
 334 volumetric repeatability; in this case, the MT volumetric repeatability is within 2  $\mu\text{m}$ . This means  
 335 that either the backlash error or the repeatability itself are within this value.

336 For the systematic error contributor ( $u_b$ ) assessment, the proposed methodology depicted in  
 337 Figure 1 was applied. In addition, a reliable tactile probe calibration was performed prior to the on-  
 338 MT measurement exercise to avoid systematic errors due to the probe set-up process. The  
 339 repeatability of the calibrated ring measurement is within  $1\ \mu\text{m}$ , which is similar to the MT  
 340 repeatability. In this manner, it was considered to be within the measurement procedure  
 341 uncertainty ( $u_p$ ) on the uncertainty budget. Figure 9 shows a comparison of the systematic error  
 342 assessment for the ISO 15530-3 technical specification and the VDI 2617-11 guideline. The difference  
 343 between both approaches is within  $1.5\ \mu\text{m}$ .



344  
 345 **Figure 9.** Systematic error ( $u_b$ ) assessment according to ISO 15530-3 technical specification and VDI  
 346 2617-11 guideline.

347 For the measurement procedure uncertainty ( $u_p$ ), results obtained from the ISO 15530-3-based  
 348 experimental test were considered because they do not require a calibrated workpiece. Here, it is  
 349 crucial to understand the effect of temperature gradients on the results. Thus, the experimental test  
 350 suggests on-MT measurements immediately after the machining process of the workpiece replica  
 351 standard and measurements under a no-load condition when the temperature on the MT side and  
 352 workpiece side is constant at  $20\ ^\circ\text{C}$ . The temperature variation on the on-MT measurement scenario  
 353 is within  $3\ ^\circ\text{C}$ , and the workpiece temperature increases to  $22.5\ ^\circ\text{C}$  (on average) immediately after  
 354 the machining process, after which it stabilises to  $19.5\ ^\circ\text{C}$  (on average) after an on-MT measurement  
 355 acquisition time of 2h. Figure 10 shows the measurement procedure uncertainty ( $u_p$ ) for each  
 356 measurement feature, both for measurements executed immediately after the machining process as  
 357 well as measurements executed under no-load conditions [4].



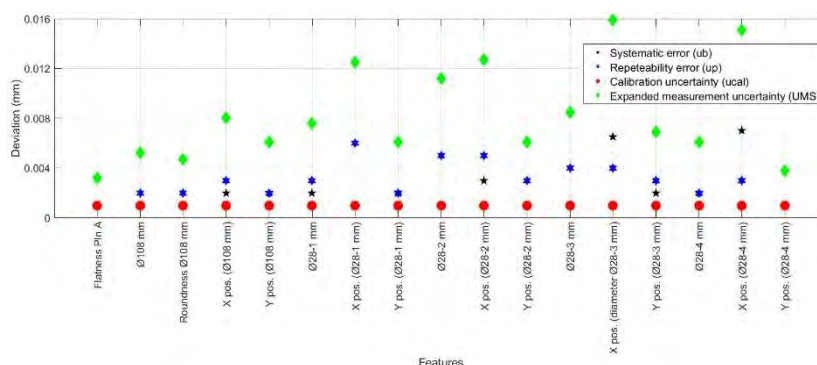
358  
 359 **Figure 10.** Measurement procedure uncertainty ( $u_p$ ) results for both approaches. [4]

360 The measurement procedure uncertainty results ( $u_p$ ) show differences between the  
 361 measurement executed under the no-load condition and the measurements executed immediately  
 362 after the machining process. All of the results show repeatability within  $6\ \mu\text{m}$  for the no-load  
 363 condition, while the maximum repeatability values for the measurements immediately after the  
 364 machining process are within  $10\ \mu\text{m}$ . The form error feature measurement (flatness and roundness)  
 365 shows better measurement procedure uncertainty results than the scale-related feature  
 366 measurement (diameter and positioning values) because these features are more sensitive to the

367 measurement scenario temperature variation [34]. Here, factors such as the swarf or dirty surfaces  
 368 should affect the  $u_p$  uncertainty result.

369 For the uncertainty ( $u_{cal}$ ) contributor, the volumetric error mapping of the MT also indicates the  
 370 uncertainty of the volumetric measurement exercise; it is obtained using a Monte-Carlo simulation  
 371 technique considering the spatial displacement measurement uncertainty for the laser tracer NG, U  
 372 ( $k = 2$ ) =  $0.2 \mu\text{m} + 0.3 \mu\text{m}/\text{m}$  [33]. The obtained uncertainty contributor ( $u_{cal}$ ) of the volumetric error  
 373 mapping is within  $1 \mu\text{m}$ .

374 Finally, the uncertainty budget of the task-specific uncertainty assessment in shop floor  
 375 conditions according to the VDI 2617-11 guideline [3] is depicted in Figure 11. Similar to the ISO  
 376 15530-3 technical specification, the expanded measurement uncertainty results were obtained using  
 377 Equation 2 for a coverage factor of  $k = 2$ , where  $u_{MS}$  is given by Equation 1. For the measurement  
 378 procedure uncertainty ( $u_p$ ), the contribution to the uncertainty budget uncertainty results for the  
 379 no-load condition were considered.



380

381 **Figure 11.** Uncertainty budget according to VDI 2617-11 guideline (no-load condition).

382 Finally, Table 1 shows the uncertainty budget assessment within the VDI 2617-11 guideline  
 383 and it is compared with the result obtained according to the ISO 15530-3 technical specification.

384 **Table 1** Uncertainty budget according to VDI 2617-11 guideline and comparison with ISO 15530-3 technical  
 385 specification. (results in  $\mu\text{m}$ )

Feature	$u_b$	$u_p$	$u_{cal}$	$u_{MS}$	$U_{MS} - \text{VDI 2617-11}$	$U_{MS} - \text{ISO15530-3}$
Flatness Plan A	1.0	0.7	1.0	1.6	3.2	3.9
Ø108 mm	1.0	2.2	1.0	2.6	5.2	4.9
Roundness Ø108 mm	1.0	1.9	1.0	2.4	4.7	4.7
X position (Ø108 mm)	2.0	3.3	1.0	4.0	8.0	8.0
Y position (Ø108 mm)	2.0	2.1	1.0	3.1	6.1	5.6
Ø28-1 mm	2.0	3.1	1.0	3.8	7.6	8.4
X position (Ø28-1 mm)	1.0	6.1	1.0	6.3	12.5	13.2
Y position (Ø28-1 mm)	2.0	2.1	1.0	3.1	6.1	5.7
Ø28-2 mm	1.0	5.4	1.0	5.6	11.2	10.9
X position (Ø28-2 mm)	3.0	5.5	1.0	6.3	12.7	14.3
Y position (Ø28-2 mm)	1.0	2.7	1.0	3.0	6.1	7.3
Ø28-3 mm	1.0	4.0	1.0	4.2	8.5	8.4
X position (Ø28-3 mm)	6.5	4.5	1.0	8.0	15.9	17.9
Y position (Ø28-3 mm)	2.0	2.6	1.0	3.4	6.9	6.9
Ø28-4 mm	2.0	2.1	1.0	3.1	6.1	5.9
X position (Ø28-4 mm)	7.0	2.7	1.0	7.6	15.1	15.6
Y position (Ø28-4 mm)	1.0	1.3	1.0	1.9	3.8	4.3

386 Experimental results show that the uncertainty budget according to the VDI 2617-11 guideline  
 387 obtains similar results to what obtained according to the ISO 15530-3 technical specification, where  
 388 a calibrated workpiece is employed for the purpose. For the systematic error contributor ( $u_b$ ), the  
 389 difference between both approaches is within 1.5  $\mu\text{m}$ , which agrees with the accuracy of the  
 390 volumetric error mapping performance, i.e. roughly 1  $\mu\text{m}$ , and also with the backlash error, which  
 391 is within the 2  $\mu\text{m}$  result that shows the volumetric repeatability. In addition, the calibration  
 392 component ( $u_{\text{cal}}$ ) is similar in both cases because of the employed reference standards, whether the  
 393 calibrated workpiece or the volumetric error mapping solution have a similar uncertainty  
 394 contributor. For the measurement procedure contributor ( $u_p$ ), the same raw data is employed.

## 395 6. Conclusions and future work

396 This paper presents an alternative on-MT uncertainty assessment methodology based on the  
 397 VDI 2617-11 guideline, which could allow scaling traceable on MT measurements to large-size MTs.  
 398 The current approach, which is based on the ISO 15530-3 technical specification, requires a  
 399 calibrated workpiece, which is similar to the manufactured part. Therefore, the solution is not very  
 400 flexible, especially for larger parts, for which it is tedious and expensive. In addition, it also presents  
 401 the two main alternatives for the adoption of the volumetric error mapping technology to MTs.

402 An experimental uncertainty budget of on-MT measurement was presented:

- 403 • Making a comparison with the ISO 15530-3 technical specification, the systematic error  
 404 contributor ( $u_b$ ) on the VDI 2617-11 guideline is shown to be affected by those error sources:  
 405 the geometric error of the MT, probing system, workpiece under measurement,  
 406 measurement procedure and the geometric error mapping technique.
- 407 • The random contributor ( $u_p$ ) comprises the MT repeatability, touch probe repeatability, and  
 408 temperature variation in the measurement scenario. For the experimental approach, the  
 409 measurement procedure and the workpiece under measurement were not considered in the  
 410 uncertainty budget because an easy-to-measure medium size prismatic component was  
 411 measured. Moreover, negligible deformations occur during the clamping process.  
 412 Furthermore, the probing system characterisation and the uncertainty of the volumetric  
 413 error mapping technique are within 2  $\mu\text{m}$ . The former is considered within the procedure  
 414 uncertainty contributor ( $u_p$ ) and the latter is considered as the  $u_{\text{cal}}$  contributor.

415 The experimental exercise which was performed without a calibrated workpiece shows that  
 416 the obtained results are similar to what was obtained using a calibrated workpiece. For the  
 417 systematic error contributor ( $u_b$ ), the difference between both approaches is within 1.5  $\mu\text{m}$ , which is  
 418 similar to the volumetric error mapping uncertainty, for which the difference is approximately 1  
 419  $\mu\text{m}$ , and also with the volumetric repeatability of the MT, which includes the backlash error within  
 420 2  $\mu\text{m}$ . Random errors for both experimental approaches are the same because they were obtained  
 421 on the ISO 15530-3 approach.

422 In summary, the methodology offers an opportunity to obtain traceable CMM measurements  
 423 on MTs without employing a calibrated workpiece as long as interferometer-based technology is  
 424 developed for MT volumetric error mapping and calibration.

425 The results obtained were validated on a three linear axis medium-size MT owing to machine  
 426 availability and other practical issues. The future work will focus on scaling the presented  
 427 methodology to large MTs similar to those used in large-scale manufacturing; the ISO 15530-3  
 428 approach is not affordable because a calibrated workpiece similar to the manufactured part is  
 429 required, which makes the solution difficult and expensive.

430 In this scenario, this research work is a gateway to large on-MT traceable measurement.

431

432 **Author Contributions:** I.V. and E.G.-A. contributed to the MT volumetric error mapping assessment. A.S.  
 433 contributed to the execution of the on-MT measurement in shop floor conditions. J.A.Y.F contributed to the  
 434 manuscript. U.M. led the research work and contributed significantly to the paper. All authors contributed to  
 435 the editing of the manuscript.

436 **Conflicts of Interest:** The authors declare no conflict of interest.

437 **References**

- 438 [1] Schmitt R, Peterek M. Guidelines for traceable measurements on machine tools. 11th Int. Symp. Meas.  
439 Qual. Control 2013, Sept. 11-13, 2013, Cracow-Kielce, Pol., 2013, p. 11–4.
- 440 [2] Schmitt R, Peterek M. Traceable measurements on machine tools-Thermal influences on machine tool  
441 structure and measurement Uncertainty. *Procedia CIRP* 2015;33:576–80.  
442 doi:10.1016/j.procir.2015.06.087.
- 443 [3] Mutilba U, Gomez-Acedo E, Kortaberria G, Olarra A, Yagüe-Fabra JA. Traceability of On-Machine  
444 Tool Measurement: A Review. *MDPI Sensors* 2017;17:40. doi:10.3390/s17071605.
- 445 [4] Mutilba U, Sandá A, Vega I, Gomez-acedo E, Fabra JAY. Traceability of on-machine tool measurement:  
446 Uncertainty budget assessment on shop floor conditions. *Measurement* 2019;135.  
447 doi:10.1016/j.measurement.2018.11.042.
- 448 [5] Flack D. Measurement Good Practice Guide No. 42: CMM verification. 2001.
- 449 [6] ISO. ISO 10360-2:2009. Geometrical product specifications (GPS) -- Acceptance and reverification tests  
450 for coordinate measuring machines (CMM) -- Part 2: CMMs used for measuring linear dimensions.  
451 2009.
- 452 [7] ISO. ISO 10360-1, Geometrical Product Specifications (GPS) -- Acceptance and reverification tests for  
453 coordinate measuring machines (CMM) -- Part 1: Vocabulary. 2000.
- 454 [8] ISO. ISO/TS 15530-3: 2004. Geometrical Product Specifications (GPS) — Coordinate measuring  
455 machines (CMM): Technique for determining the uncertainty of measurement — Part 3: Use of  
456 calibrated workpieces or standards. 2004.
- 457 [9] ISO. ISO/TS 15530-4:2008. Geometrical Product Specifications (GPS) — Coordinate measuring  
458 machines (CMM): Technique for determining the uncertainty of measurement — Part 4: Evaluating  
459 task-specific measurement uncertainty using simulation. 2008.
- 460 [10] Verein Deutscher Ingenieure (VDI). VDI/VDE 2617-11-Accuracy of Coordinate Measuring Machines -  
461 Characteristics and Their Checking - Determination of the Uncertainty of Measurement for Coordinate  
462 Measuring Machines Using Uncertainty Budgets. 2011.
- 463 [11] ISO. ISO 230-10:2016. Test code for machine tools -- Part 10: Determination of the measuring  
464 performance of probing systems of numerically controlled machine tools. 2011.
- 465 [12] ISO. ISO 230-7: 2015, Test code for machine tools -- Part 7: Geometric accuracy of axes of rotation. 2015.
- 466 [13] ISO. ISO 230-2: Test code for machine tools — Part 2: Determination of accuracy and repeatability of  
467 positioning of numerically controlled axes. 2014.
- 468 [14] ISO (Technical comitee ISO/TC 39/SC 2). ISO 230-4:2005, Test Code for MTs. Part 4. Circular Tests for  
469 Numerically Controlled machine tools. 2005.
- 470 [15] ISO (Technical comitee ISO/TC 39/SC 2). ISO 230-6:2002, Test Code for Machine tools. Part 6.  
471 Determination of Positioning Accuracy on Body and Face Diagonals (Diagonal Displacement Tests).  
472 2002.
- 473 [16] ISO (Technical comitee ISO/TC 39/SC 2). ISO 230-1:2012, Test code for machine tools -- Part 1:  
474 Geometric accuracy of machines operating under no-load or quasi-static conditions. 2012.
- 475 [17] ISO. JCGM 100:2008 (GUM 1995 with minor corrections). Evaluation of measurement data — Guide to  
476 the expression of uncertainty in measurement. 2008.
- 477 [18] Nisch S, Schmitt R. Production integrated 3D measurements on large machine tools. LVMC Large Vol.  
478 Metrol. Conf. 2010, Chester, 2010.
- 479 [19] Holub M, Jankovych R, Andrs O, Kolibal Z. Capability assessment of CNC machining centres as  
480 measuring devices. *Meas J Int Meas Confed* 2018;118:52–60. doi:10.1016/j.measurement.2018.01.007.
- 481 [20] Trapet E. Traceability of Coordinate Measurements According to the Method of the Virtual Measuring  
482 Machine: Part 2 of the Final Report Project MAT1-CT94-0076. vol. Volumen 35. 1999.
- 483 [21] Kupiec R, Krawczyk M. Virtual Coordinate Measuring Machine Built Using Lasertracer System and  
484 Spherical Standard. *Metrol Meas Syst* 2013. doi:10.2478/mms-2013-007.
- 485 [22] Sladek, J, Gasca. A. Evaluation of coordinate measurement uncertainty with use of virtual machine  
486 model based on Monte Carlo method. *Measurement* 2012;45:1564–75.
- 487 [23] Slocum A. Precision machine-design - Macromachine Design Philosophy and its applicability to the  
488 design of Micromachines. IEEEMEMS '92, proceedings. An Investig. Micro Struct. Sensors, Actuators,  
489 Mach. Robot. IEEE, 1992. doi:10.1109/MEMSYS.1992.187687.
- 490 [24] Mathworks. Matlab software 2018.
- 491 [25] Mathworks. Least sqaues plane fitting code 2018.
- 492 [26] Schmitt R, Peterek M, Quinders S. Concept of a Virtual Metrology Frame Based on Absolute  
493 Interferometry for Multi Robotic Assembly 2014;m:79–86.
- 494 [27] Schwenke H. The latest trends and future possibilities of volumetric error compensation for machine

- 495 tools. 15th Int. Mach. Tool Eng. Conf. IMEC, Tokyo, Japan, 2-3 Novemb., 2012, p. 57–71.
- 496 [28] Schwenke H, Knapp W, Haitjema H, Weckenmann A, Schmitt R, Delbressine F. Geometric error  
497 measurement and compensation of machines—An update. *CIRP Ann - Manuf Technol* 2008;57:660–75.  
498 doi:10.1016/j.cirp.2008.09.008.
- 499 [29] Schwenke H, Schmitt R, Jatzkowski P, Warmann C. On-the-fly calibration of linear and rotary axes of  
500 machine tools and CMMs using a tracking interferometer. *CIRP Ann - Manuf Technol* 2009;58:477–80.  
501 doi:10.1016/j.cirp.2009.03.007.
- 502 [30] Mutilba U, Yagüe-Fabra JA, Gomez-Acedo E, Kortaberria G, Olarra A. Integrated multilateration for  
503 machine tool automatic verification. *CIRP Ann* 2018;67:555–8. doi:10.1016/j.cirp.2018.04.008.
- 504 [31] Schmitt R, Peterek M, Morse E, Knapp W, Galetto M, Härtig F, et al. Advances in Large-Scale  
505 Metrology – Review and future trends. *CIRP Ann - Manuf Technol* 2016. doi:10.1016/j.cirp.2016.05.002.
- 506 [32] ISO 10791-7:2014. Test conditions for machining centres -- Part 7: Accuracy of finished test pieces. 2014.
- 507 [33] Schwenke H, Franke M, Hannaford J, Kunzmann H. Error mapping of CMMs and machine tools by a  
508 single tracking interferometer. *CIRP Ann - Manuf Technol* 2005;54:475–8. doi:10.1016/S0007-  
509 8506(07)60148-6.
- 510 [34] Mutilba U, Sandá A, Vega I, Gomez-acedo E, Bengoetxea I, Yagüe JA. Traceability of on-machine tool  
511 measurement : Uncertainty budget assessment on shop floor conditions. *Measurement* 2019;135:180–8.  
512 doi:10.1016/j.measurement.2018.11.042.
- 513